Journal of Materials Chemistry B

Materials for biology and medicine

www.rsc.org/MaterialsB

Volume 1 | Number 11 | 21 March 2013 | Pages 1511–1650

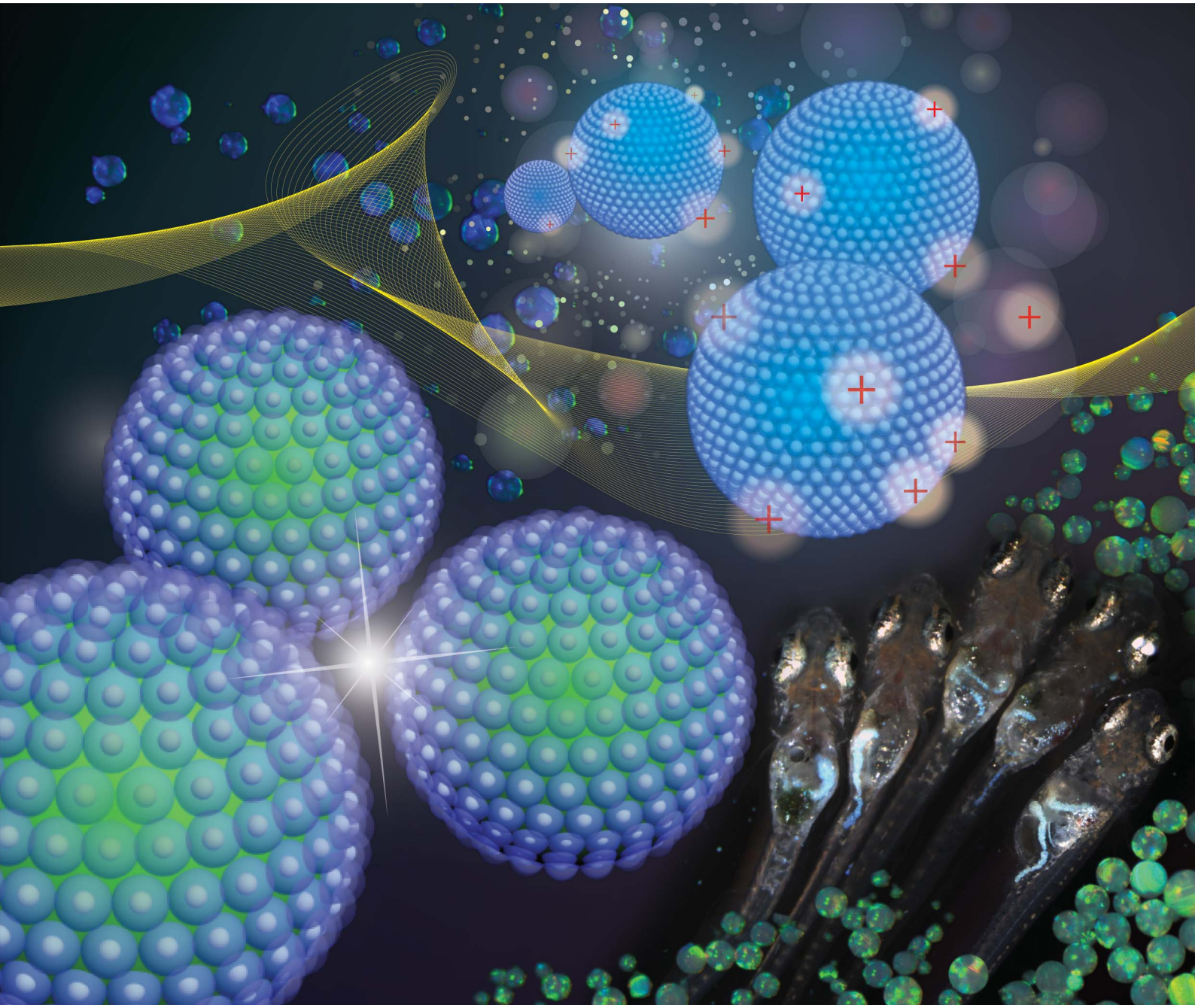

ISSN 2050-750X

RSC Publishing

PAPER

Zhicheng Zhang, Michael Hon-Wah Lam *et al.*

Non-invasive *in vivo* imaging of the ionic regimes along the gastrointestinal tract of a freshwater vertebrate model organism (Japanese medaka) using responsive photonic crystal beads

2050-750X(2013)1:11;1-0

Published on 07 January 2013. Downloaded by Shenzhen Institute of Advanced Technology, CAS on 2/6/2023 6:26:02 AM.

Journal of Materials Chemistry B

RSC Publishing

PAPER

View Article Online
View Journal | View Issue

Cite this: *J. Mater. Chem. B*, 2013, **1**, 1535

Non-invasive *in vivo* imaging of the ionic regimes along the gastrointestinal tract of a freshwater vertebrate model organism (Japanese medaka) using responsive photonic crystal beads

Xuemin Du,[abc] Ngai-Yu Lei,[c] Hiu-Man Chiu,[c] Xuewu Ge,[ab] Zhicheng Zhang*[ab] and Michael Hon-Wah Lam*[ac]

Received 11th October 2012
Accepted 3rd January 2013

DOI: 10.1039/c2tb00236a

www.rsc.org/MaterialsB

Microspherical photonic colloidal crystalline beads that are responsive to media ionic strength of cationic electrolytes have been developed for *in vivo* imaging of the morphology and concentration gradient of cationic electrolytes along the gastrointestinal (GI) tract of live Japanese medaka (*Oryzias latipes*). These responsive photonic beads were assembled from core–shell nano-sized particles with polystyrene-*co*-polyacrylic acid (PS-*co*-PAA) cores and poly(hydroxyethyl methacrylate-*co*-p-styrene sulfonate) (PHEMA-*co*-PSS) hydrogel shells. The three-dimensional orderly packing of these nano-sized core–shell particles gave rise to the photonic properties of the resultant colloidal crystalline array of microspheres. The cationic electrolyte-induced volume phase transition of the sulfonate-laden hydrogel shells of the nano-sized particles altered the lattice spacing among those particles and brought about the photonic responses of the colloidal crystalline beads. Unambiguous changes in the diffraction colour of the colloidal crystalline beads were observable under ordinary ambient light in solution media of increasing concentration of sodium chloride up to 500 mM. These photonic colloidal crystalline beads were found to possess enough structural integrity for *in vivo* imaging of the GI tract of live Japanese medaka. With the use of a conventional optical microscope, the gradient in the ionic strength of cationic electrolytes along the GI tract of live Japanese medaka larvae was readily revealed, with a lower electrolyte concentration in the mid-intestine (<50 mM) compared to that of the posterior-intestine (≥50 mM). Our results demonstrated the potential of stimuli-responsive photonic materials in bio-imaging applications.

Introduction

Electrolyte homeostasis refers to mechanisms with which living organisms maintain optimal electrolyte concentrations in their body fluids so as to sustain proper metabolic activities.[1] Sodium, potassium and calcium cations, together with chloride anion, play vital roles in the functioning of the neural system, preservation of acid–base balance, and the regulation of osmotic pressure of body fluids.[2] For those organisms that thrive in environments where the concentration and the composition of the media electrolytes are far from optimal, electrolyte homeostasis is even more crucial for their survival. In freshwater fish, this is achieved through numerous processes. These include the absorption of electrolytes from the surrounding media through active processes predominantly at the gills, and the regulation of selective re-absorption of ions along the gastrointestinal (GI) tract.[3–6] While the physiological roles of the GI tract in freshwater teleosts in electrolyte homeostasis during digestion have been well studied, they were mainly revealed by dissection and measurement of the concentration of selective ions in the recovered chyme along the tract.[7] It would be nice if those data obtained can be correlated with the actual ionic strength along the GI tract of live fish. However, such *in vivo* measurements of electrolyte concentration in the fish gut are very difficult, if not impossible, to carry out without suitable *in vivo* imaging tools.

The orderly assembling of monodispersed, inert nano-sized particles into closely packed three-dimensional lattices can generate intriguing photonic band-gap phenomena owing to the Bragg diffraction of visible and near-infrared (NIR) radiation of specific wavelengths by the lattices. If the photonic band-gap properties of such materials can be made responsive toward specific external stimuli, they can be very useful chemosensors. Indeed, Holtz and Asher[8] have pioneered this idea and reported

[a]*Advanced Laboratory for Environmental Research & Technology, USTC-CityU, Suzhou, China*

[b]*Department of Polymer Science and Engineering, University of Science & Technology of China, Hefei, Anhui, China. E-mail: zczhang@ustc.edu.cn; Fax: +86 551 5320512; Tel: +86 0551 3601597*

[c]*State Key Laboratory for Marine Pollution, Department of Biology and Chemistry, City University of Hong Kong, Tat Chee Ave., Kowloon, Hong Kong SAR, China. E-mail: bhmhwlam@cityu.edu.hk; Fax: +852 3442 0522; Tel: +852 3442 7329*

Published on 07 January 2013. Downloaded by Shenzhen Institute of Advanced Technology, CAS on 2/6/2023 6:26:02 AM.

a series of stimuli-responsive polymerized colloidal crystal array (PCCA) thin films. In recent years, the application of responsive photonic materials for chemosensing has been extended rapidly to cover the sensing of pH,[9] temperature,[10] magnetic field strength,[11–13] metal ions,[14] glucose,[15] and selected biomolecules and metabolites.[16] Advantageous features offered by these new photonic chemosensors include (1) photonic bandgap properties (*e.g.* diffraction wavelength and colour) can be conveniently fine-tuned; (2) unlike ordinary luminescent detection, changes in photonic properties can be readily observed under ambient light, and the intensity of the photonic Bragg diffraction (and hence, the chemosensing response) increases with ambient light illumination; and (3) biocompatible and biodegradable materials can be used for the construction of the photonic crystalline lattices. While these chemosensing potentials of stimuli-responsive photonic bandgap materials have captured much research attention, attempts to apply these materials in *in vivo* sensing and bio-imaging are scarce. In this work, we developed specific microspherical photonic colloidal crystalline beads for the *in vivo* imaging of the gradient in the ionic strength of cationic electrolytes along the GI tract of a teleost model organism – Japanese medaka (*Oryzias latipes*). These photonic beads were assembled from specially designed core–shell hydrogel nano-sized particles, in which the swelling properties of the hydrogel coatings were responsive to the media ionic strength of cationic electrolytes.

Experimental

Materials

Styrene (St) and acrylic acid (AA) were purchased from Aldrich, and were distilled under vacuum before use. Potassium persulfate (KPS) was purchased from Aldrich, and was recrystallized before use. Sodium *p*-styrene sulfonate (SSS) was obtained from Alfa, and was used as received. Divinylbenzene (DVB) was obtained from Aldrich. Hydroxyethyl methacrylate (HEMA), hexadecene (HE), and *N*,*N*′-methylenebisacrylamide (NMBA) were obtained from Acros. Hypermer 2296 was obtained from Croda. They were all used as received. All other reagents were of analytical grade and were used as received. Double-distilled water was used in all the experiments.

Instrumentation

Electron microscopy (SEM and TEM) was carried out on a Philips XL30 ESEM-FEG environmental scanning electron microscope (SEM) and a FEI/Philips Tecnai 12 Bio TWIN transmission electron microscope (TEM), respectively. Photographs of the photonic colloidal crystalline beads were taken with an optical microscope (Olympus BX60) equipped with a CCD camera (Media Cybernetics Evolution MP 5.0). Photonic beads were illuminated by white light focused through an objective (20×, NA = 0.40) onto the samples. Reflectance spectra of the photonic beads in the range 400–750 nm were measured by coupling the microscope to a Princeton Instrument SpectraPro 2300i spectrometer *via* an optical lens and a light guide. For the *in vivo* imaging of Japanese medaka, *Oryzias latipes*, a Leica M205 FA motorized fluorescence stereomicroscope, equipped with a DCF 310 FX CCD camera, with a lower magnification enabling the capturing of the whole body images of the fish larvae was used.

A Malvern Zetasizer Nano ZS instrument was used in particle size and zeta potential measurements, at 25 °C, of the core–shell nano-sized particles.

Preparation of the monodispersed core–shell nano-sized particles and the microspherical photonic crystal beads

Monodispersed core–shell nano-sized particles were prepared by seeded copolymerization of HEMA and SSS on nano-sized PS-*co*-PAA seeds using KPS as an initiator in a three-necked round flask with a reflux condenser and a mechanical stirrer. A typical synthesis of the core–shell nanoparticles was as follows: 5.3 g of St, 0.55 g of DVB, and 0.6 g of AA were dissolved in 100 mL of distilled water in a 250 mL round flask. When the mixture was refluxed at 100 °C for 3 min, polymerization was initiated by the addition of 5 mL of aqueous solution containing 62.7 mg of KPS. After the reaction mixture for preparing PS-*co*-PAA seeds was kept for 2 h under constant stirring, certain aqueous mixture containing 3.0 g of HEMA, 0.2 g of SSS, 0.013 g of NMBA and 24 mg of KPS was added. The polymerization was allowed to continue for another 3 h at 100 °C. The resulting core–shell nanoparticles were collected by centrifugation at 15 500 rpm for 3 × 20 min.

Core–shell nano-sized particles without the sulfonate functional moiety in the hydrogel shells were prepared in a similar way as described above, except that no SSS was used in the fabrication.

The procedure adopted for the fabrication of the photonic colloidal crystalline beads was as follows: an aqueous suspension (1 mL) containing 4.0 wt% of the monodispersed core–shell nanoparticles was dropped into a test tube filled with 15 mL of hexadecene as an oil phase and an amphiphilic block copolymer, Hypermer 2296 (2.0 wt%), as a stabilizer. The resultant latex suspension in the test tube was then broken up into droplets by vigorous hand-shaking, followed by pouring into a 15 cm diameter glass Petri dish, which had been treated with octadecyltrichlorosilane to render its inner wall hydrophobic. The suspension in the glass Petri dish was warmed to 50 °C for 72 h to allow the water within these droplets to slowly evaporate. During the evaporation, the core–shell nanoparticles were self-assembled into microspherical orderly packed lattices. These resultant microspherical photonic crystal beads were collected and thoroughly washed with *n*-hexane to remove the hexadecene, followed by freeze-drying to obtain the photonic crystal beads in the dried form.

Control photonic colloidal crystalline beads that were not responsive to media ionic strength were fabricated in a similar way as described above, except that core–shell nano-sized particles without the sulfonate functional moiety in the hydrogel shells were used instead.

Measurement of reflectance spectra of the photonic crystal beads and *in vivo* imaging of freshwater medaka (*Oryzias latipes*)

Photonic crystal beads were suspended in aqueous buffers of pH 6 and pH 9 with various concentrations of NaCl from 10 mM

 This journal is © The Royal Society of Chemistry 2013

Published on 07 January 2013. Downloaded by Shenzhen Institute of Advanced Technology, CAS on 2/6/2023 6:26:02 AM.

to 500 mM. These suspensions were dropped onto microscope slides, covered with coverslips and were then immediately used for microscopy observation, photography and measurement of reflectance spectra.

The embryos of *Oryzias latipes* were obtained from Dr Doris W. T. Au (City University of Hong Kong). Hatched larvae were maintained in an embryo rearing medium (2 mM NaCl). Larvae (5 day-post-hatch, *ca.* 4–5 mm in length) were placed in a 96-well cell culture plate and exposed to photonic beads in the embryo rearing medium. In each of the cell culture wells, one medaka larva was incubated with a suspension of 1.0 mg of photonic crystal beads for 24 h. The larvae were then transferred into the well of depression microscope slides and turned, with the help of a dropper, so that their dorsal side was facing upward for microscope imaging. And the RGB value was measured with Photoshop CS2.

Results and discussion

Fig. 1a and b show typical TEM images of the monodispersed core–shell nano-sized particles with a diameter of *ca.* 187 nm. The specially designed core–shell nanoparticles with carboxylate-functionalized polystyrene (PS-*co*-PAA) as cores and poly(hydroxyethyl methacrylate-*co*-*p*-styrene sulfonate) (PHEMA-*co*-PSS) as shells were fabricated by emulsifier-free emulsion polymerization.[17] The zeta potential of these nano-sized particles was -70.0 ± 0.82 mV in Milli-Q water. Fig. 1c and d shows a typical spherical photonic colloidal crystalline bead assembled from the closely packed core–shell nano-sized particles. These assembled microspherical beads were polydispersed (Fig. 1e and f), with 49% of the beads in the 20–30 μm range.

The incorporation of sulfonate functionalities into the hydrogel shell of the nano-sized particles gives rise to the responsive shrinking properties of these particles toward media ionic strength. Table 1 tabulates the changes in the hydrodynamic particle size (D_z) of these core–shell nano-sized particles with media ionic strength (mediated by the addition of NaCl) in both acidic and basic buffers. The decrease in D_z of the nano-sized particles with increasing NaCl concentration is generally independent of media pH. The resultant photonic colloidal crystalline beads assembled from these core–shell nanoparticles display characteristic photonic properties that are also responsive toward media ionic strength (Scheme 1 and Fig. 2). With the increasing concentration of NaCl up to 500 mM, the photonic diffraction λ_{max} of the colloidal crystalline beads blueshifted from 548 nm to 506 nm at pH 6 (from 550 nm to 506 nm at pH 9) (Fig. 3). This manifested in a gradual change of their diffraction colour from glossy green to violet. This responsive phenomenon is attributable to the shrinking of the hydrogel coatings of the core–shell nano-sized particles that were assembled into the photonic crystal beads due to the

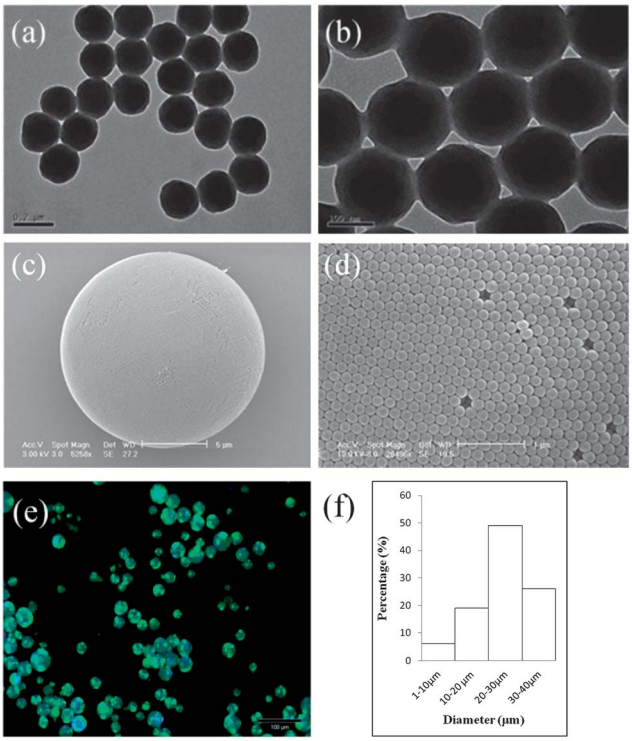

Fig. 1 Microspherical ionic strength-responsive photonic colloidal crystalline beads: (a) and (b) TEM images of the monodispersed core–shell nano-sized particles of diameter 187 nm; (c) SEM image of an assembled colloidal crystalline bead; (d) surface morphology of a colloidal crystalline bead; (e) a typical optical microscope image of the photonic beads suspended in rearing medium illuminated by white light focused through the objective (20×, NA = 0.40); (f) size distribution of the beads obtained by optical microscopy.

Table 1 Average hydrodynamic diameter (D_z) and polydispersity index (PDI) of the core–shell nano-sized particles in buffers at pH 6 and 9 with various concentrations of NaCl from 10 mM to 500 mM

	pH 6		pH 9	
NaCl (mM)	D_z (nm)	PDI	D_z (nm)	PDI
10	266 ± 1.3	0.014	267 ± 2.2	0.012
50	250 ± 4.2	0.016	252 ± 2.3	0.009
154	240 ± 3.6	0.013	242 ± 2.5	0.014
500	238 ± 2.2	0.008	237 ± 3.6	0.015

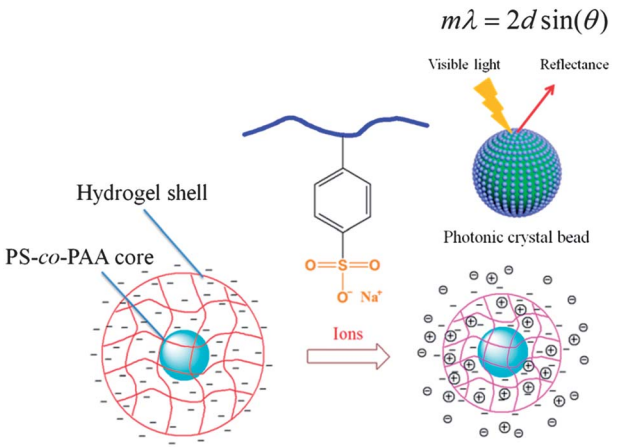

Scheme 1 Schematic illustration of the responsive mechanism of the core–shell hydrogel nano-sized particles towards media ionic strength.

Published on 07 January 2013. Downloaded by Shenzhen Institute of Advanced Technology, CAS on 2/6/2023 6:26:02 AM.

volume phase transition behavior of their PHEMA-*co*-PSS hydrogel shells brought about by the lowering of the internal osmotic pressure of the hydrogel resulting from the decrease of the electrostatic repulsion between the anionic sulfonate functionalities as more sodium cations entered the hydrogel layer.[9,18] This reduced the mean separation among the nano-sized particles in the crystalline lattice and shifted the photonic diffraction to shorter wavelengths.

Besides the ionic strength-responsive colloidal crystalline beads, we have also fabricated control beads from similar core–shell nano-sized particles that contained no PSS in the hydrogel shell. With the lack of sulfonate functionalities, these nano-sized particles did not possess responsive properties toward media ionic strength. The colloidal crystalline beads assembled from them did not show any response in terms of their photonic diffraction colour toward media ionic strength. These control beads were used alongside the responsive beads in our *in vivo* imaging experiments.

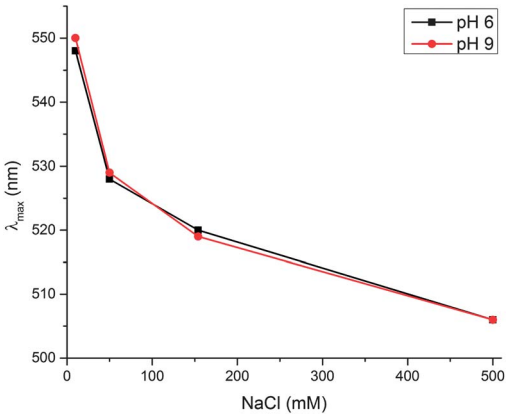

Fig. 3 The change of photonic diffraction λ_{max} of the responsive photonic colloidal crystalline beads with various concentrations of NaCl at different pH.

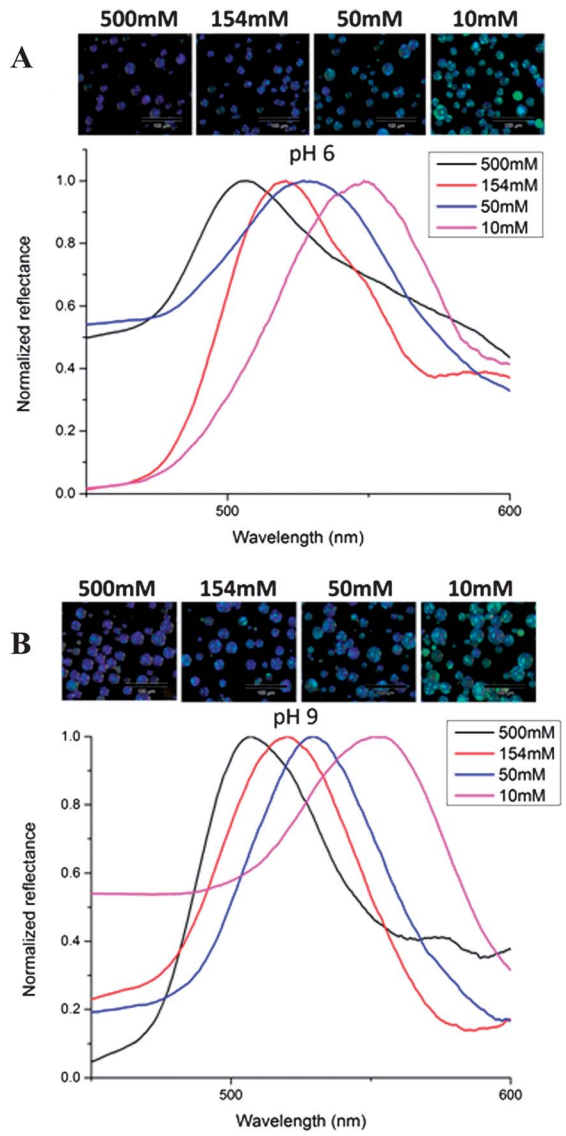

Fig. 2 Reflectance spectra of the photonic colloidal crystalline beads in pH 6 (A) and pH 9 (B) buffers with various concentrations of NaCl from 10 mM to 500 mM. From left to right, the color of the beads changes from glossy green to purple with increasing media ionic strength.

Japanese medaka (*Oryzias latipes*), a unique vertebrate model, is a small fish that enables high resolution (<1 μm) *in vivo* imaging of biological structures and functions at virtually all levels of organization, from subcellular to gross anatomical.[19–21] It is known that they do not have a stomach and pylorus.[22] The oesophagus is connected to the mid-intestine, which coils into loops. It is the major site for food digestion and absorption, as well as for the absorption of ions for electrolyte homeostasis. We fed both the responsive and control photonic colloidal crystalline beads to medaka larvae (5-dph, average length *ca.* 4–5 mm) kept in freshwater culture media (2 mM NaCl) in 96-well cell culture plates. Visual indication of accumulation of these photonic beads in their GI tracts was

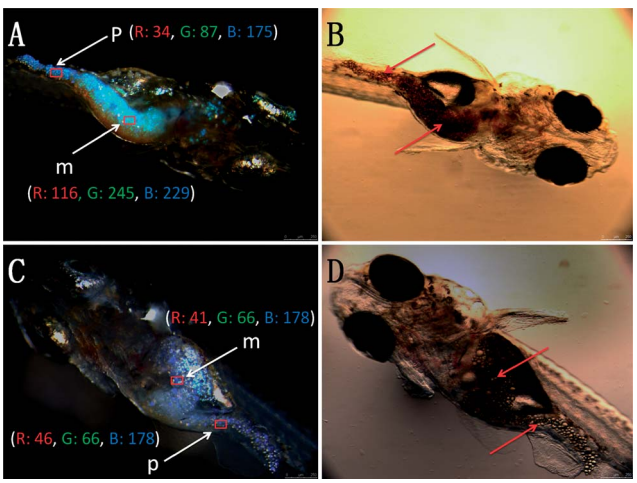

Fig. 4 *In vivo* imaging of the GI tract of a live freshwater medaka (*Oryzias latipes*) larva by the photonic colloidal crystalline beads revealing the morphology of the looped mid-intestine (m) and the posterior-intestine (p), as well as the change in ionic strength along the GI tract (corresponding RGB triplets are shown in brackets). The upper images (A and B) were obtained using responsive photonic beads, while the lower images (C and D) were obtained using control beads that are not responsive towards media ionic strength.

This journal is © The Royal Society of Chemistry 2013

Published on 07 January 2013. Downloaded by Shenzhen Institute of Advanced Technology, CAS on 2/6/2023 6:26:02 AM.

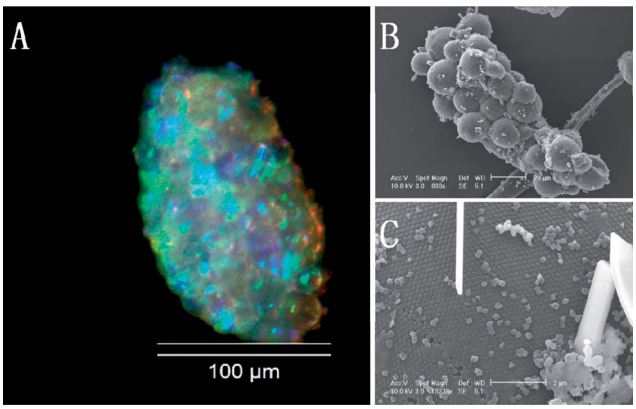

Fig. 5 Microscope images of excreted colloidal crystalline beads: (A) a typical dark-field image illustrating the retention of photonic properties of an excreted bead; (B) and (C) SEM images of the excreted beads demonstrating the structural integrity of the photonic crystalline beads for *in vivo* imaging under conditions as harsh as the peristaltic movement of the gut.

observable after 24 h (Fig. 4). The larvae remained energetic after two weeks of exposure. Photonic properties of both the responsive and control beads were retained within the GI tract, indicating that they were structurally intact under the peristaltic squeezing of the intestine of the organism. Even after passing through the GI tract, the excreted beads retained their orderly packed structure and photonic properties (Fig. 5).

Previous works[23] on electrolyte homeostasis of freshwater teleosts have already hinted that they are always in a hyper-osmotic state with respect to their surrounding environment. This can result in the loss of ions by diffusion and a gain of water by osmosis. To counter these effects, salt is actively re-absorbed by the gills, and excess water is eliminated through the production of large amounts of diluted urine.[24,25] As ambient water is ingested along with food, the digestive tract becomes an important component in osmoregulation – *via* the absorption of ions in the intestine.[26]

Fig. 4 shows typical *in vivo* optical microscope images of the GI tract of Japanese medaka larvae revealed by the responsive (Fig. 4A and B) and control (Fig. 4C and D) colloidal crystalline beads. From the photonic diffraction colour, the fluid phase of the digestion segment (mid-intestine (m)) contained a significantly lower concentration of cationic electrolytes than the posterior intestine (p). This corresponds well to post-mortem measurements obtained from *Hassar* and silver catfish.[27] Taking the sodium ion as an example, its electrochemical potential is governed by the activity of Na^+- and K^+-ATPases in the enterocytes.[28] The activity of these Na^+- and K^+-ATPases in freshwater teleosts is known to be higher in the anterior intestine than in the posterior intestine, resulting in the lower concentration of Na^+ ions in the mid-intestine.[29,30] This is vividly demonstrated in Fig. 4A. Glossy green diffraction colour (R: 116, G: 245, B: 229) was observed in the mid-intestine of Japanese medaka larvae, while a blue diffraction (R: 34, G: 87, B: 175) was observed in the posterior-intestine. On the other hand, control photonic colloidal crystalline beads fabricated from core–shell nano-sized particles without sulfonates in their hydrogel coating showed similar photonic diffraction colour along the GI tract. According to the photonic responses of the responsive photonic beads depicted in Fig. 2, the ionic strength of cationic electrolytes in the mid-intestine of Japanese medaka larvae should be <50 mM, while that in the posterior-intestine ≥50 mM.

Conclusions

To conclude, we have developed an optical bio-image technique for the *in vivo* visualization of the ionic strength along the gastrointestinal tract (GI) of live Japanese medaka based on ionic strength-responsive photonic colloidal crystalline beads. The volume–phase transition of the *p*-styrenesulfonate-based hydrogel coatings on the core–shell nano-sized particles compiling the photonic colloidal crystalline beads has given rise to their responsive properties. This specially designed photonic bio-imaging tool possessed enough structural integrity for *in vivo* imaging under conditions as stringent as the peristaltic movement of the intestine, and showed virtually no toxicity to the test animals. We hope to show that the application of stimuli-responsive photonic band-gap materials in bio-imaging is an area worthy of exploring.

Acknowledgements

The work described in this paper was supported by the Centre for Functional Photonics of the City University of Hong Kong. Xuemin Du acknowledges the National Natural Science Foundation of China (no. 51073146, 51103143, 51173175) and the Joint PhD Scheme of the University of Science & Technology of China and the City University of Hong Kong. Special thanks are given to Dr Doris Au of the Department of Biology & Chemistry, City University of Hong Kong, for the provision of Japanese medaka larvae.

Notes and references

1 J. Ballantyne and J. Robinson, *J. Comp. Physiol., B*, 2010, **180**, 475–493.
2 S. R. Verma, S. Rani and R. C. Dalela, *Toxicol. Lett.*, 1981, **9**, 327–332.
3 B. Baldisserotto, C. Kamunde, A. Matsuo and C. M. Wood, *Comp. Biochem. Physiol., Part C: Toxicol. Pharmacol.*, 2004, **137**, 363–372.
4 B. Baldisserotto, M. J. Chowdhury and C. M. Wood, *Aquat. Toxicol.*, 2005, **72**, 99–117.
5 A. Becker, J. Gonçalves, M. M. Burns, J. Vieira, J. Radünz Neto and B. Baldisserotto, *Fish Physiol. Biochem.*, 2012, **38**, 1001–1017.
6 K. Dabrowski, C. Leray, G. Nonnotte and D. A. Colin, *Comp. Biochem. Physiol., Part A: Mol. Integr. Physiol.*, 1986, **83**, 27–39.
7 C. Bucking and C. M. Wood, *Am. J. Physiol.: Regul., Integr. Comp. Physiol.*, 2006, **291**, R1764–R1772.
8 J. H. Holtz and S. A. Asher, *Nature*, 1997, **389**, 829–832.
9 K. Lee and S. A. Asher, *J. Am. Chem. Soc.*, 2000, **122**, 9534–9537.

Published on 07 January 2013. Downloaded by Shenzhen Institute of Advanced Technology, CAS on 2/6/2023 6:26:02 AM.

10 T. Kanai, D. Lee, H. C. Shum and D. A. Weitz, *Small*, 2010, **6**, 807–810.
11 J. P. Ge, Y. P. Hu, T. R. Zhang, T. Huynh and Y. D. Yin, *Langmuir*, 2008, **24**, 3671–3680.
12 J. P. Ge, Y. X. Hu and Y. D. Yin, *Angew. Chem., Int. Ed.*, 2007, **46**, 7428–7431.
13 J. P. Ge and Y. D. Yin, *Adv. Mater.*, 2008, **20**, 3485–3491.
14 S. A. Asher, A. C. Sharma, A. V. Goponenko and M. M. Ward, *Anal. Chem.*, 2003, **75**, 1676–1683.
15 M. Ben-Moshe, V. L. Alexeev and S. A. Asher, *Anal. Chem.*, 2006, **78**, 5149–5157.
16 A. C. Sharma, T. Jana, R. Kesavamoorthy, L. Shi, M. A. Virji, D. N. Finegold and S. A. Asher, *J. Am. Chem. Soc.*, 2004, **126**, 2971–2977.
17 Z. Z. Gu, H. H. Chen, S. Zhang, L. G. Sun, Z. Y. Xie and Y. Y. Ge, *Colloids Surf., A*, 2007, **302**, 312–319.
18 J. H. Holtz, J. S. W. Holtz, C. H. Munro and S. A. Asher, *Anal. Chem.*, 1998, **70**, 780–791.
19 Y. Wakamatsu, S. Pristyazhnyuk, M. Kinoshita, M. Tanaka and K. Ozato, *Proc. Natl. Acad. Sci. U. S. A.*, 2001, **98**, 10046–10050.
20 R. C. Hardman, D. C. Volz, S. W. Kullman and D. E. Hinton, *Anat. Rec.*, 2007, **290**, 770–782.
21 D. E. Hinton, Y. Wakamatsu, K. Ozato and S. Kashiwada, *Comp. Hepatol.*, 2004, **3**(suppl. 1), S30.
22 D. Kobayashi, T. Jindo, K. Naruse and H. Takeda, *Dev., Growth Differ.*, 2006, **48**, 283–295.
23 B. Baldisserotto, Osmoregulatory adaptations of freshwater teleosts, in *Fish Adaptations*, ed. A. L. Val and B. G. Kapoor, Science Publishers, Enfield, 2003, pp. 179–201.
24 C. M. Wood, Toxic responses of the gill, in *Target organ toxicity in marine and freshwater teleosts: organs*, ed. D. Schlenk and W. H. Benson, Taylor & Francis, London, 2001, vol. 1, pp. 1–89.
25 B. J. Curtis and C. M. Wood, *J. Exp. Biol.*, 1991, **155**, 567–583.
26 B. Baldisserotto and O. M. Mimura, *Comp. Biochem. Physiol., Part A: Mol. Integr. Physiol.*, 1994, **108**, 297–302.
27 A. G. Becker, J. F. Gonçalves, L. O. Garcia, E. R. Behr, F. J. K. Mallmann, D. L. Graça and B. Baldisserotto, *Fish Physiol. Biochem.*, 2006, **32**, 105–112.
28 J. L. Specker, K. Sundell, M. Chandlee and B. Soffientino, *Fish Physiol. Biochem.*, 2000, **23**, 159–164.
29 S. S. Madsen, S. D. McCormick, G. Young, J. S. Endersen, R. S. Nishioka and H. A. Bern, *Fish Physiol. Biochem.*, 1994, **13**, 1–11.
30 C. Nielsen, S. S. Madsen and B. Th. Björnsson, *J. Fish Biol.*, 1999, **54**, 799–818.

 This journal is © The Royal Society of Chemistry 2013